

AUTOMATED ROUTE PLANNING FOR CONSTRUCTION SITE UTILIZING BUILDING INFORMATION MODELING

SUBMITTED: July 2021

REVISED: July 2022

PUBLISHED: August 2022

EDITOR: Žiga Turk

DOI: [10.36680/j.itcon.2022.040](https://doi.org/10.36680/j.itcon.2022.040)

*Ankan Karmakar, Ph.D. Student,
Department of Civil Engineering, Indian Institute of Technology Bombay;
204046006@iitb.ac.in*

*Abhishek Raj Singh, Research Associate,
Department of Civil Engineering, Indian Institute of Technology Bombay;
arsingh@iitb.ac.in*

*Venkata Santosh Kumar Delhi, Associate Professor,
Department of Civil Engineering, Indian Institute of Technology Bombay;
venkatad@iitb.ac.in*

SUMMARY: Construction Vehicle route planning forms a significant component of Construction Site Layout Planning (SLP). At present, the construction industry has no standard method of planning vehicle routes resulting in chaotic situations on sites. The study proposes an integration of optimization techniques with Building Information Modeling (BIM) to generate feasible routes taking into account the dynamic nature of construction projects. A systematic workflow is developed for the integration of these platforms. The steps involved in the process are presented through a case study highlighting a decision support system for project planners. The advantages of sensitivity analysis alongside a visual interpretation of the construction routing schedule are achieved through the integrated workflow. Thus, the developed workflow provides an approach to enhance the efficiency of daily equipment movements at the site by reducing the possible conflicts and enhancing accessibility. Though the study limits itself in handling the internal vehicular movements, the developed workflow could be extended to manage the project supply chain; moreover, the site personnel movements could be integrated to provide a safer work environment at the construction site.

KEYWORDS: Accessibility, Site route planning, Multi-objective optimization, Dijkstra's algorithm, Building information modeling (BIM), 4D construction schedule

REFERENCE: Ankan Karmakar, Abhishek Raj Singh, Venkata Santosh Kumar Delhi (2022). Automated route planning for construction site utilizing Building Information Modeling. *Journal of Information Technology in Construction (ITcon)*, Special issue: 'The Eastman Symposium', Vol. 27, pg. 827-844, DOI: [10.36680/j.itcon.2022.040](https://doi.org/10.36680/j.itcon.2022.040)

COPYRIGHT: © 2022 The author(s). This is an open access article distributed under the terms of the Creative Commons Attribution 4.0 International (<https://creativecommons.org/licenses/by/4.0/>), which permits unrestricted use, distribution, and reproduction in any medium, provided the original work is properly cited.

1. INTRODUCTION

Construction projects are dynamic, having facilities and routes changing over time depending on the project phases. A survey poll shows that the movement of plants, operatives, and materials accounts for nearly up to 30% of the total delay in construction work (Harris and McCaffer, 2013). Thus, optimizing routing and minimizing conflicts or congestion at the site looking towards smooth accessibility are multi-objective complex problems. The problem a planner faces while doing logistics and layout planning is how to handle a considerable number of constraints. Different factors affect the optimum travel path, such as interrelation between various facilities, dynamic site layout, loading-unloading places, dumping yard, type of roads, types of vehicles, turning radius and height constraints, and congestion (Varghese and O'Connor, 1995; Mahdjoubi and Yang, 2001). Travel path distances worked as an essential input to optimize the location of temporary facilities. Researchers addressed the problem by reducing transport costs (Mawdesley, Al-jibouri and Yang, 2002). However, the feasible route of equipment movement may not always stand out as the shortest route. Accessibility of various road sections depends on their geometry and attributes. Also, the interruption in smooth equipment movement at the site can result from conflict among traffic flows, causing blockages (Pradhananga and Teizer, 2013). Further, most of these studies are on grid-based 2D spaces, which encounters a significant challenge in visualization and data loss. The current advancements in technology have introduced Building Information Modeling (BIM) to enhance the experience, visualization, collaboration, and coordination among different project stakeholders. Integration of BIM with project management has marked the paradigm shift in the industry (Fazli *et al.*, 2014). The integrated data can be used for site routing, planning, and temporary facility planning (Le, Dao and Chaabane, 2019). According to the extant literature, accessibility is best understood utilizing simulation in virtual design and construction (Lin *et al.*, 2013; Schwabe, König and Teizer, 2016). The seamless data transfer from BIM to optimization modules can improve productivity and enhance the avoidance of accessibility problems at the site.

2. LITERATURE REVIEW

The existing literature can be divided into five categories – (i) site path planning, (ii) site accessibility, (iii) congestion at the site, (iv) BIM in site routing and layout planning, and (v) optimization algorithms for site routing.

The evaluation criteria of most site layout problems are a function of the total distance travelled. Researchers (Li and Peter E. D. Love, 1998) depicted that total travel distance is based on the trips between the existing facilities. Hence, the travel distance is nothing but a multiplication of the number of trips with distances between facilities. Similarly, (Li *et al.*, 2001) proposed a model considering material flow-time. This flow-time considers the time required for a material to pass through different areas such as entrance, storage, staging, and supply point. There are different methods used for the calculation of distances. One of these processes is rectilinear or Manhattan (Mawdesley, Al-jibouri and Yang, 2002), whereas the other method is the Euclidean distance between two points (Li and Love, 2000). However, these methods are approximate and do not give actual distance travelled at the site, as the distance generated might pass through facilities. Sanad *et al.* (2008) divided the actual distance into three parts. One is from the centroid of the facility to the access road; the second length is through the access road, and the third portion is from the access road ending point to the centroid of the site. A BIM-based route generation method was proposed through obstacle avoidance (Song and Marks, 2019). However, the study ignored the possible interaction among facilities. A more practical, realistic approach was adopted by (Benjaoran and Peansupap, 2019) as they used grids to define the actual travel distance. However, rectangular blocks do not replicate the freeform geometry of the facilities and the road networks. In addition, when the pickup and drop points are considered at the facility's boundary, it does not consistently reproduce site conditions. In the study by (Singh, Patil and Delhi, 2019), the researchers used BIM to generate the parameters for the actual travel path. Model lines were created in Revit to get the actual distances. The road network method had been used by (Varghese and O'Connor, 1995) to identify the best suitable travel path. An advantage of this method is that it can accept any freeform geometry and gives the actual path distance. However, they have not considered any inter-facility or facilities to demand points interaction. Integration of the model proposed by (Varghese and O'Connor, 1995), along with multiple sources and destinations, will help depict the complexity and dynamics to simulate a situation similar to actual site conditions. Fig. 1 depicts the methods discussed graphically.

The geometrical constraints and the load constraints restrict the access of equipment to available routes. To date, accessibility is evaluated manually with a dependence on the experience of planners in construction (Tam and Tong, 2003). The space allocation for equipment is evaluated on a site through qualitative positioning due to a

lack of intuitive tools (Akinci, Fischer and Kunz, 2002). Consequently, conflicts occur due to incorrect assignment of space to facilities or equipment. Sometimes, demolition is required for newly constructed elements to make adequate space for equipment to move freely. Also, navigating transportation paths are difficult because of convoluted routes and obstacles in the narrow work area. As a result, even minimum distances can reduce operational efficiency (Lin *et al.*, 2013). Occasionally, it can cause additional cost and damage to the project (Soltani, Tawfik and Fernando, 2002). Researchers proposed computing methods to reduce transportation time (Lam, Ning and Ng, 2007; Ning, Lam and Lam, 2010). To enhance visualization for a better understanding of accessibility, (Sadeghpour, Moselhi and Alkass, 2006) have used computer-aided tools to analyze the proper position of facilities in 2D platforms. The accessibility of equipment can be understood utilizing a simulation-based approach. Safety and accessibility are addressed in a simulation model for decision-supporting sandbox systems (Lin *et al.*, 2013). Research integrating multi-body dynamic motion of the wheel, track, and chain type machinery with optimization module, has generated suitable routes between two points (Lin, Hung and Kang, 2015). The drawbacks in previous research, which connect two points without considering the turning radius and movement of equipment, can be addressed by collision detection when shape and size are considered.

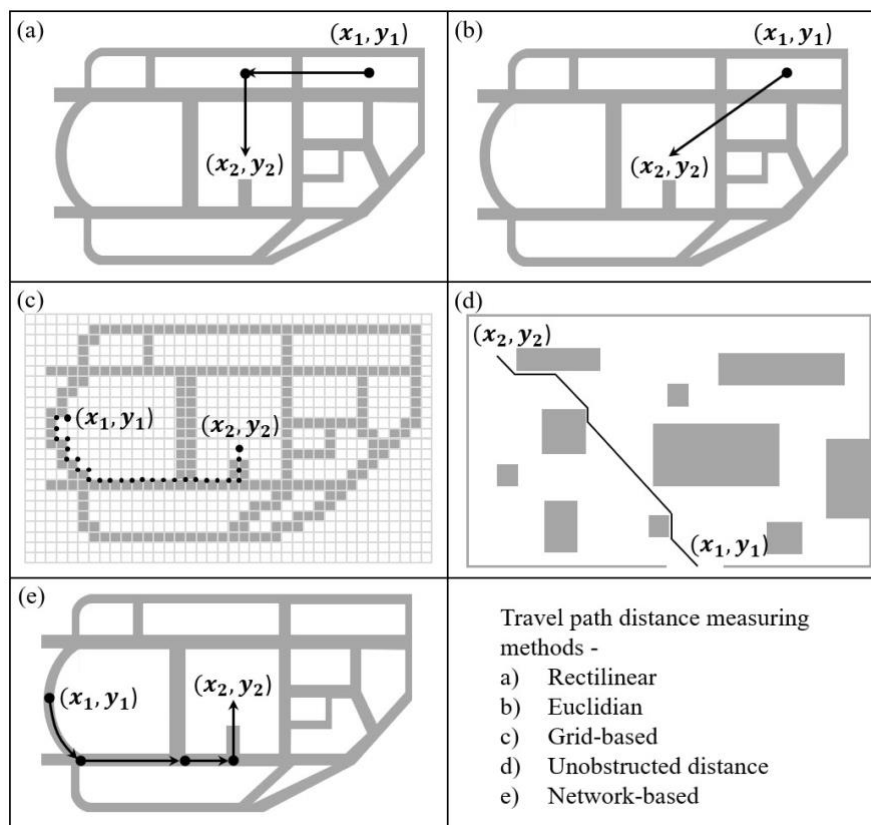


FIG. 1: Travel path distance calculating methods used by different researchers

On the other hand, multiple crews share the same working space or driveways in a construction site. Hence, congestion here is denoted by the waiting time of equipment when it has to wait for another piece of equipment to complete a task in a given space. One-third of the construction safety fatalities occur at the site due to congestion and inappropriate movement of the cranes (Neitzel, Seixas and Ren, 2001). To identify a collision and congestion-free path, researchers have used movements of crane parts through an optimization algorithm in a virtual 3D space (Ali, Babu and Varghese, 2005). A site congestion analysis on real-time data was done for site excavation activity in a cell-based simulation model through a defined congestion index (Pradhananga and Teizer, 2014). Another study was conducted to place construction equipment on the site depending on rule-based checking (Schwabe, König and Teizer, 2016). The equipment sizes and safety distances were the primary criteria to check conflicts with existing site logistics and upcoming structures to be constructed. The algorithm worked based on the collision boundaries prepared in the BIM environment. Thus, current studies show a growing inclination towards the adaptation of BIM as it helps in integrating the space management and visualization aspect.

The success of BIM over other methods is in the size of the project and its complexity (Barlish and Sullivan, 2012). BIM provides visual aids, and it also offers a paradigm to manage and store information, including geometry, properties, quantities, and spatial relationships (Zuppa, Issa and Suermann, 2009; Singh and Helander, 2016). The parametric data from BIM helped analyze the obstruction and the minimum possible travel distance between origin and destination (Song and Marks, 2019). From the perspective of layout problems, automated site layout methods for continuous space are addressed in the literature (Kumar and Cheng, 2015). Multi-objective site planning depending on coordinate systems, cost function and adjacency score (Le, Dao and Chaabane, 2019) were executed through data exchange from BIM. In case of feasibility and accessibility, collision and interference between multiple site elements, BIM provides easy understanding through clash detection and overlapping boundaries in 3D space (Schwabe, König and Teizer, 2016). An AR-enabled decision support system for site layout planning was proposed for immersive perspective exchange with the stakeholders (Singh, Karmakar and Delhi, 2020). Another essential aspect of site path planning is the time dependant behaviour of the construction site. The time dimension consideration in sites can be static, dynamic, or phases (Andayesh and Sadeghpour, 2014). 4D BIM can manage and integrate complex time-dependent variabilities with 3D model elements (Li, Xu and Zhang, 2017). BIM can handle and transfer information effortlessly across the project lifecycle (Karmakar and Delhi, 2021). Even though it makes BIM a potential candidate for route planning, it should be aided with optimization techniques to generate the optimal result.

One of the challenging issues in solving the route planning problem is the selection of solving method or algorithm. Previous works focused on the planning of construction site scenarios have targeted parameters like safety, obstacle avoidances, minimum travel cost, minimum noise pollution, visibility range, and vehicle constraints on turns. For achieving these goals with multiple constraints, the researchers have used various optimization techniques. The neural evolution through crossover in the genetic algorithm (GA) was used to locate temporary facilities (Mawdesley, Al-jibouri and Yang, 2002). Also, BIM was integrated with GA to optimize the location of temporary facilities by minimizing overall cost and distance (Singh and Delhi, 2018). In the Binary Tree Algorithm case, once all the paths are generated from source to destination, the path planning is done by avoiding obstacles from source to destination in a tangent visibility graph (Turky *et al.*, 2013). Another popular algorithm is the A* algorithm, where the heuristics function is used to estimate the lowest-cost path between start and end node with a path cost, highest visibility and lower risk (Soltani, Tawfik and Fernando, 2002). This method was further studied by integrating basic facilities geometries exported from BIM to enhance the easy flow of data in a grid-based approach (Song and Marks, 2019). Particle Swarm Optimisation (PSO) is explored on a grid-based platform of excel to calculate the travel distance by adding movement on each unobstructed block, designated as a path (Benjaoran and Peansupap, 2019). Ant colony optimization (ACO) also follows the principle of swarm intelligence to find the shortest and collision-free route, which was used in grid networks by (Brand *et al.*, 2010) for robot path planning. The comparison between GA, PSO and ACO showed PSO to be the most efficient method to reduce overall cost; however, the run time for PSO is highest amongst others for grid-based networks (Adrian, Utamima and Wang, 2015). Apart from grid-based methods, for the network-based method, Dijkstra's algorithm is used to determine the shortest route between one source and any destination for undirected graphs (Varghese and O'Connor, 1995). Among GA, A* and Dijkstra's algorithms, GA can give near-optimal solutions in less time. However, the accuracy of the solution is a significant limitation due to the greedy search techniques. As the search space increases, the time complexity becomes a significant issue for these algorithms (Soltani and Fernando, 2004). Grid-based methods on BIM tools make it challenging to accommodate irregular shapes and also increases the search space.

Hence, this study tries to integrate BIM and the network-based method with modified Dijkstra's algorithm based on the binary heap to reduce the complexity of the model and generate near-optimal solutions efficiently. Finally, this paper attempts to present a framework to address the path planning problem by minimizing internal conflicts and accessibility problems at the site. It aims to enhance the overall productivity and minimize the schedule variance through a decision support system for site logistics and planning engineers.

3. METHODOLOGY

As depicted in Fig. 2, the proposed framework requires four inputs, i.e. a building information model, construction project schedule, a database for site equipment and material location. A set of visual programming modules are carried out over the BIM model to generate the required properties for analysis. Next, a 4D schedule is auto-generated, where the system tags 3D elements to the activities. The road network parameters extracted from BIM

are fed into the optimization module. User-defined attributes from the schedule and database control the outputs from the optimization algorithm. Finally, the outputs from the process are presented in the form of textual and graphical results. The optimization process provides two sets of solutions. The single-objective function focuses on the internal movements of site equipment. On the other hand, the multi-objective function minimizes the conflicts and congestion among external supply vehicles coming to the site and the internal site movements. The methodology is further described in detail in the following sub-sections 3.1 to 3.5.

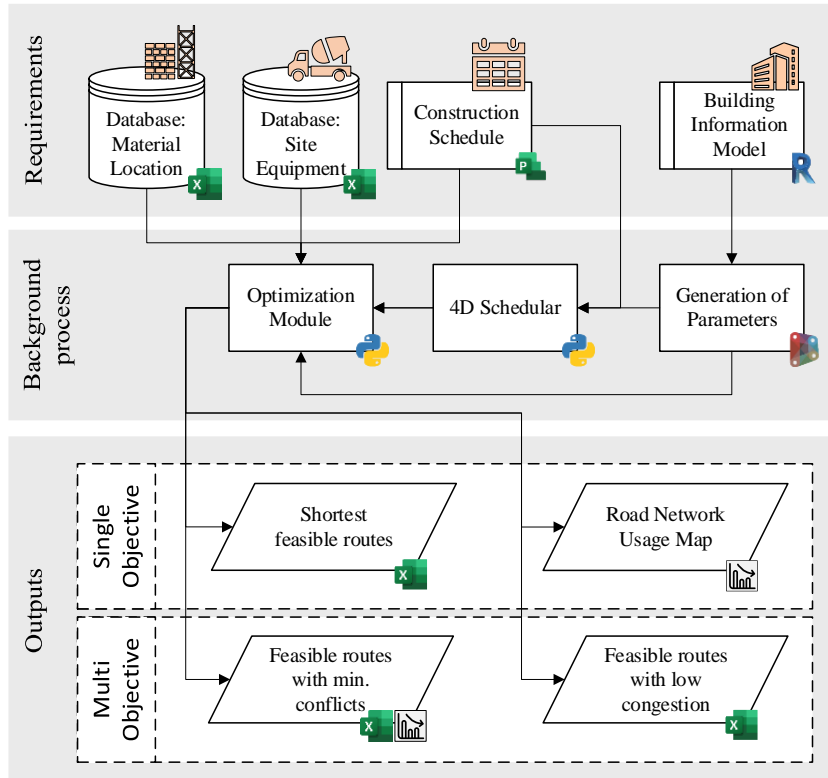


FIG. 2: Proposed site route planner framework

3.1 Creation of Building Information Model

The first step in applying the framework is to create a road network model on a BIM platform. As Autodesk Revit is one of the most used BIM platforms in the AEC industry, with an adaptation of around 46% (UNIFI, 2019), it is used in this research to provide BIM functionality. A parametric model element was created with four user-defined parameters, i.e., road width, pavement material, start node and end node. These units are repeated to create the complete road network of the site. Here, nodes(n) are defined as a point in the network where any combination of roads intersect, pavement material change or sharp turn exist. Any road segment joining between two nodes is designated as an edge(e). The model must be a LOD 300 model, as it requires specific geometry for clash detection and quantity takeoff. The structural elements should have materials such as 'concrete', 'steel', 'metal' in their names or 'class'. Two additional user-defined parameters are also required to be specified for each element, i.e., the name of the structure or 'building' and the 'zone' to which it belongs. These parameters use 'shared parameter' properties such that they can be used across projects and models.

3.2 Site Equipment and Material Location Database

A database of pre-defined construction equipment is created with parameters such as pavement type (where the movement of that equipment is restricted), the hauling capacity of the vehicle, the unit of hauling capacity, speed in km/hr, length, and breadth of the vehicle. All possible locations for temporary facilities are populated and assigned in the first iteration by heuristics for the material location database. Next, the user can choose the equipment type for each TFs from the given database. The hauling capacities correspond to the choice of equipment. The hauling capacity of the vehicle is also a parameter that the user can choose. The hauling capacity of the vehicle governs the succeeding equipment parameters such as speed, length, and breadth.

3.3 Generation of Parameters from BIM

A visual programming platform, Dynamo, is used to generate the parameters from Revit. Visual coding is used to generate properties from the road network, quantify structural elements, and produce overhead clash reports for temporary roads based on user inputs.

The road network parameters consist of three user-defined parameters, six geometry related parameters and unique element id. The start node, end node, and pavement material drive the user parameters. The start and endpoints of each segment, alongside their length and width, are the geometric parameters. The structural elements are classified into five major types, i.e., beam, column, floor, foundation and wall. An example of the floor formwork calculation formula is given in Equation 1. In the equation, F_s represents the total formwork area of the slab. t_s is the thickness of the slab, and P_s , A_s are the perimeter and area of slab derived from Revit built-in property. f is a gate parameter, which is 0 for slab-on-grade or concrete on metal deck, and it is 1 for elevated concrete slabs. The other properties exported through quantification are element id, structure name, building zone, material, and volume.

$$F_s = t_s \times P_s + A_s \times f \quad (1)$$

Overhead clash problems include roads that might lose their ability to accommodate traffic once any structure gets built above or near their proximity. The creation of temporary routes is a ubiquitous practice at construction sites. The temporality of the road may depend upon its overhead or edge boundary constraint. Fig. 3 demonstrates an example of a temporary road where the structure gets constructed later during the project life cycle. The clash of road segments with structural elements is determined based on the minimum overhead clearance assigned by the user. The accessibility duration of these roads is analysed according to the 4D schedule.

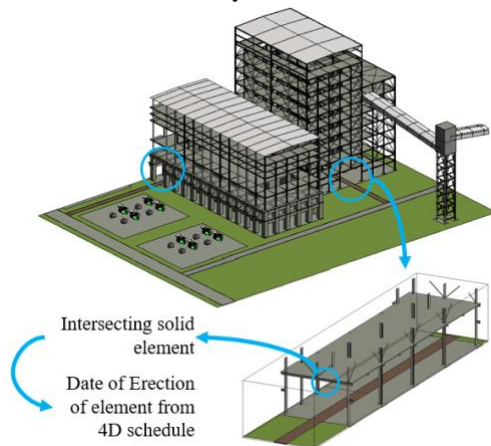


FIG. 3: Example of the temporary roads at a construction site

3.4 Construction Schedule and 4D Scheduler

A 5-level hierarchy is followed to create the schedule. The work breakdown structure (WBS) specified by the user must be maintained throughout the project schedule to maintain consistency while integrating it with the optimization module. An example of hierarchy level or WBS is summarised below:

- Level 1: Master Project (e.g., ABC Thermal Power Plant Project)
- Level 2: Buildings / Different structures (e.g., Building A, Cooling tower etc.)
- Level 3: Zones / Units / Areas (e.g., Zone C, Unit 3 etc.)
- Level 4: Materials / Supply points (e.g., Reinforcement, Concreting, Excavation etc.)
- Level 5: Level of structure (e.g., Ground floor, 7th floor etc.)

The construction schedule exported from any available scheduling software is integrated with 3D model elements from BIM to generate a 4D schedule. However, the process of attaching elements is tedious and requires custom rule creation from the user. Further changes in the schedule may lead to data loss in this process. Hence, an automated process of attaching elements to the tasks is developed. The algorithm checks through properties of elements such as building zone, level, and materials, subsequently attaching them to activity in the schedule according to the properties. Multiple elements can be tagged to a task, and conversely, elements can be tagged to multiple tasks. This attachment process is done from bottom to top. Properties such as shutter area, rebar volume

and concrete volume attach only to relevant tasks with the same names such as ‘concrete’ or ‘reinforcement’, which are then rolled up.

3.5 Optimization Module

The optimization module functions based on Dijkstra's shortest path algorithm to solve the multi-objective problem of feasible distance versus minimum conflict and feasible distance versus the avoidance of highly populated roads in the site. Both these objectives are developed over the primary focus of generating feasible routes based on the accessibility. However, the inputs required for the optimization module are gathered based on specific queries. As exhibited in Fig. 4, the user is asked to specify any date in the project start date and end date range. All the movement of construction equipment on the site is calculated based on this user-defined check date. The check date looks into the construction schedule and filters the activities running on that specified date at the lowest hierarchy level. The script then crawls through the hierarchy level of each activity to develop a list of ongoing activities. For example, if a reinforcing activity is scheduled during the check date, the list is created as ['WBS Code', 'Ground Level', 'Reinforcement', 'Zone B', 'Building 1']. As different work can proceed at different site locations, date checking ensures that the variability due to construction phases is considered. Next, after sorting, a dictionary is generated according to supply and demand points. Here, the dictionary keys are the unique materials, and delivery points correspond to the keys. This method takes care of the multiple delivery points scenario. According to the ongoing activity, WBS Code data stored in the dictionary helps locate the structural elements and get their quantification values.

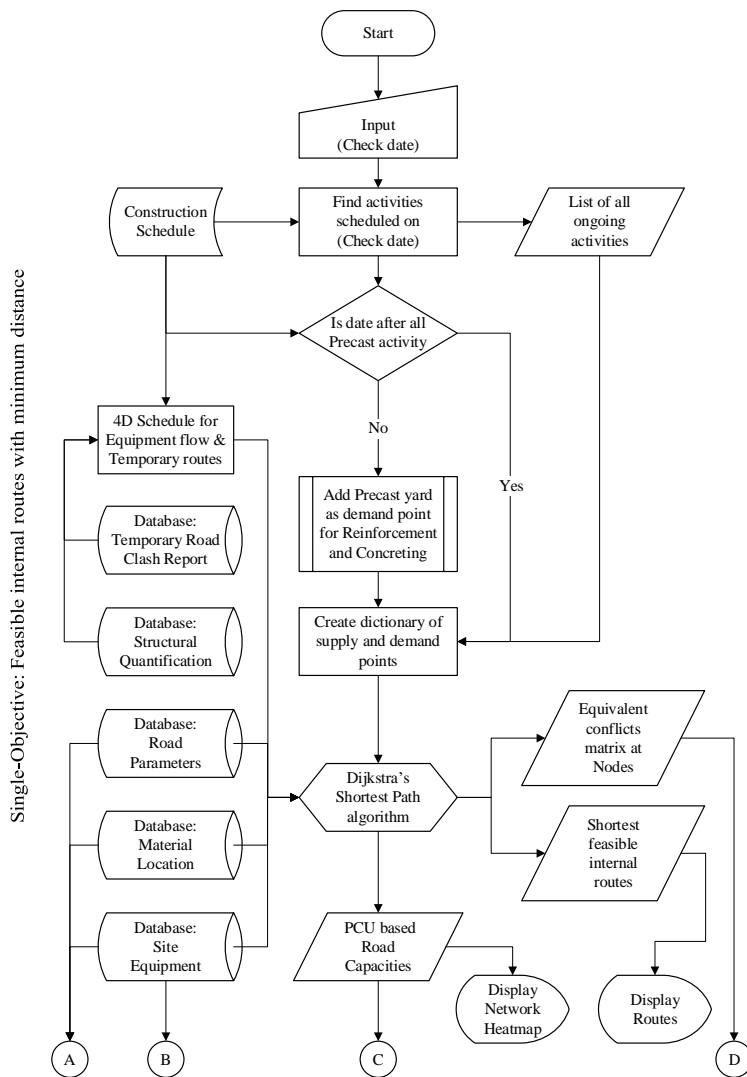


FIG.4a: Schematic representation of the background process

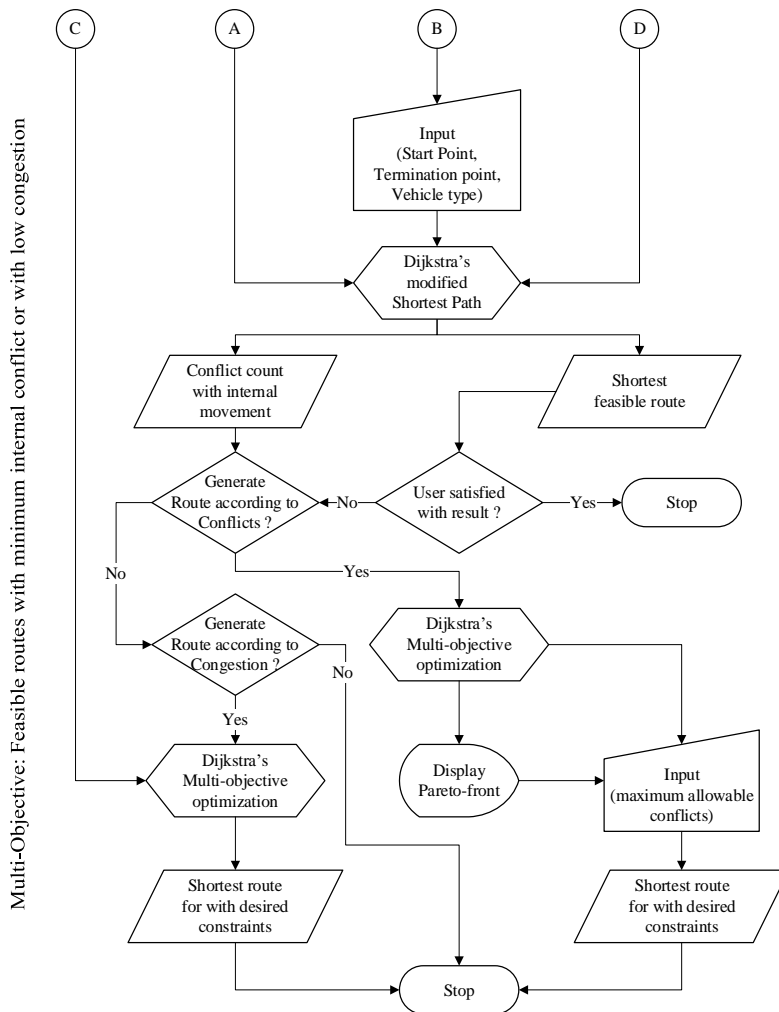


FIG. 4b: Schematic representation of the background process

A rule-based check for precast activity is applied after that. It is assumed that if the check date is after all precast activities in the site, no additional changes are required to the existing supply and demand points dictionary. However, if the check date is on or before any precast erection activity on site, the precast yard is considered one of the demand points for reinforcement and concrete. Hence, the precast yard is appended in values of demand points for 'Reinforcement' and 'Concrete' yards. Once the supply and demand points are finalized, the data is fed into the optimization module. The optimization module integrates with all other databases created (site equipment, material location and road network). The Dijkstra algorithm runs and generates the shortest route for each supply and demand point combination, given that the minimum road width and pavement type requirement are satisfied from the site equipment database. The algorithm runs based on an adjacency matrix generated from the road network database and priority queueing. The route generation algorithm draws values from the report of temporary roads clashes. While generating the graph for Dijkstra, a new parameter is added to each edge of the graph, denoted as the route's validity. The validity of the route depends upon two criteria. One of them is the road's availability due to overhead clearance and the other due to any reason leading to traffic blockage in that section. For the first criteria, the algorithm takes the element id of each road section into account and runs through the clash report to get the structural elements that might possess a barrier to that segment. The programme then loops through all the activities attached to those structural elements and notes the starting dates of those activities. If any activity has a start date before the checking date specified, it means construction over that road segment has already started, and the availability of that road segment is no more. While creating the graph, these roads become nullified, and traffic can never run through those roads. The schematic representation of the road elimination process is shown in Fig. 5.

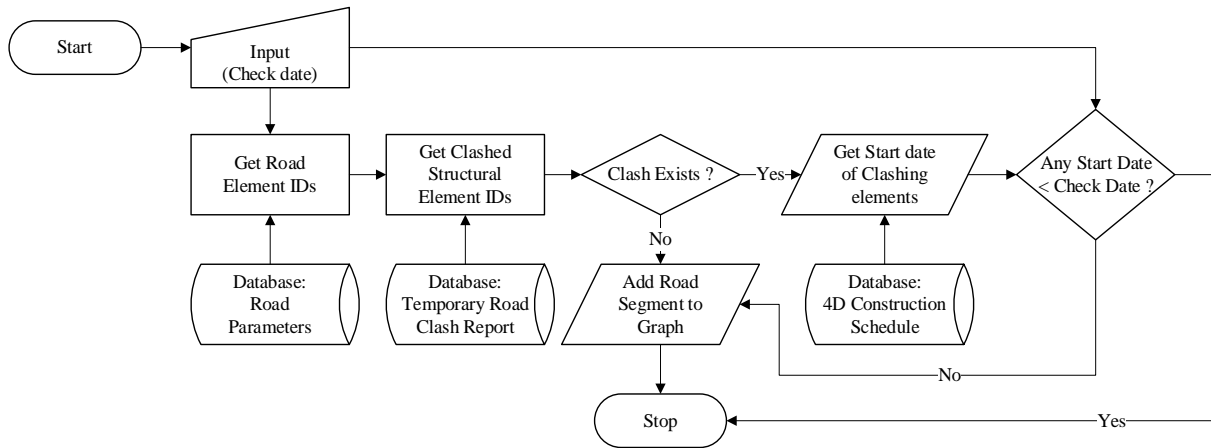


FIG. 5: Schematic representation of road elimination process for temporary roads

The second output from the initial run is the internal conflicts count matrix. The nodes that fall in the path of any equipment movement is counted as the PCU (passenger car unit) of that equipment. The starting and terminating nodes for any equipment are ignored from this calculation. If multiple vehicles move through the same nodes at the site, the count for that node is done based on equivalent passenger car units. The third output from the initial run is the flow density of equipment through road segments. The flow density is calculated based on the moving vehicle properties, the material it is carrying, the demand of that material at the destination, and the activity duration. For a particular source to demand material flow condition, the quantity of material movement (Q) and duration (D) of activity is obtained from the quantification output of the 4D schedule. The total quantity of material associated with the activity is divided by duration to obtain per day flow. The number of vehicles required per day is obtained by dividing this flow value by the vehicle's hauling capacity (H). As the vehicle size and speed vary highly in a construction site, converting the equipment to a comparable unit is necessary. For normalization, the value obtained by dividing with hauling capacity is multiplied by the PCU of the equipment. The quantity of material can vary from sqm. in case of shuttering to cum. in case of concrete. The conversion factor (c) depends on the unit of hauling capacity, as the capacity can be in weights (kg) or volume (cum.). The density (ρ) of material is required to be multiplied when hauling capacity is in weight. The formula for normalized flow (NF) calculation is shown in Equation 2. After each iteration, if any vehicle is passing through a segment of the road, the NF values are added to the total flow (TF) values of that segment, as shown in Equation 3. Here, 'x' denotes a particular road segment, 's' and 'd' denotes the sources and destination points of delivery, and 'i' and 'j' denotes the flow of delivery from any particular source to any particular delivery point through segment 'x'. The summation is multiplied by 2 to consider both way flow.

$$NF = \left[\frac{Q \times c \times \rho}{D \times H} \right] \times PCU \quad (2)$$

$$TF^x = 2 \times \sum_{j=1}^d \sum_{i=1}^s NF_{ij}^x \quad (3)$$

The construction site's internal movements are considered to be the movement of equipment required for scheduled construction. However, apart from these movements, several other travels occur at the site. Examples can be shifting of storage materials internally, shifting of temporary facilities, and stock supply to the facilities. The main objective of the second module is to determine the minimum route for these movements based on maximum allowable conflict with the internal movements or with maximum allowed congestion concerning peak traffic flow at the site. The user specifies the start and terminating point of any such movement at the beginning of the multi-optimization module. The user also selects a vehicle and its corresponding hauling capacity from the existing database. The constraint and vehicle-specific values are extracted accordingly. Once the new route is generated, each node travelled is marked as 1, and non-visited nodes are kept as 0 in the matrix 'X'. The total conflict count (cc) in a route is the product of matrix 'X' and PCU equivalent (PCU_{eq}) at the nodes connecting the route, as shown in Equation 4. 'k' represents the nodes visited among all possible 'n' nodes in a route. The total count of conflicts (cc) is an integer value. An equivalent PCU is proposed for this problem, as shown in Equation 6. In this equation, the calculated equivalent passenger car unit is represented by ' PCU_{eq} '. ' PCU_i ' and ' $Flow_i$ ' are 'passenger car unit'

for vehicle 'i' and 'flow' of vehicle type 'i' through a specific node. The PCU of construction equipment is calculated according to the Indian Highway Capacity Manual (CSIR, 2017).

$$cc = \sum_{k=1}^n X_k \times PCU_{eq_k} \quad (4)$$

$$X_k = \begin{cases} 0, & \text{if node not visited} \\ 1, & \text{if node visited} \end{cases} \quad (5)$$

$$PCU_{eq} = \sum_{i=1}^n \left[\left(\frac{PCU_i \times Flow_i}{\sum_{i=1}^n PCU_i \times Flow_i} \right) \times PCU_i \right] \quad (6)$$

The result produced in the first run is the minimum route that might have many conflicts. Hence, if the user wants a different solution with fewer conflicts, then the algorithm re-runs and generates all solutions for conflicts count zero to 'cc' obtained at Equation 4. The result is displayed in the form of Pareto front between feasible distances and conflicts counts. However, if the user opts for a minimum route based on traffic volume at road segments, a flow density map is created at the end of the first objective. For this method, the user is asked to specify the maximum percentage of peak flow volume to be disregarded when navigating the route for external equipment. For example, say the maximum PCU flowing that day at the site is 500, and the user specifies the maximum amount to be 60% of the highest value. Then all the routes above 300 PCU become invalid for the external equipment. The shortest route available, where movement is not restricted for the external vehicle, gets generated in the next step.

Both traffic flow in road segments and conflict count is derived from the 4D schedule of the site. Hence, the outcomes from these can be compared. Fig. 6 illustrates an example of how the traffic flow and conflict count are interrelated with each other for some hypothetical case. This diagram gives a holistic idea of how the different modules help each other achieve the target and depict their essentiality.

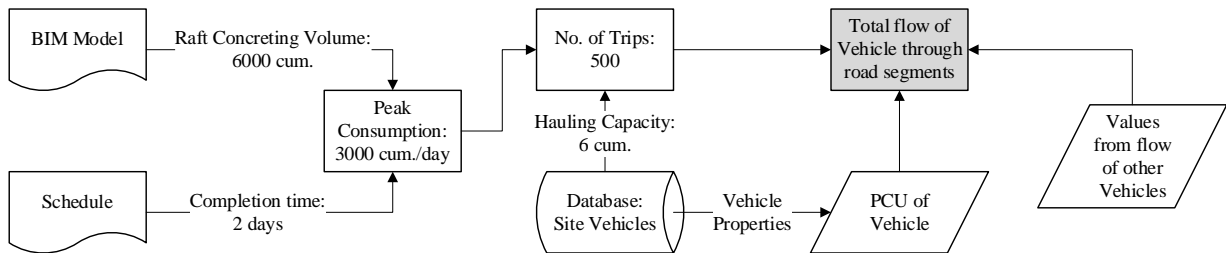


FIG. 6: Visual representation of interrelation among 4D schedule, internal conflicts and traffic flow

4. CASE STUDY

This section describes how the model is implemented in a hypothetical case study of a thermal power plant expansion project. The data, collected and used, follows an existing real-life project. However, minor modifications were carried out to diversify the testing conditions.

4.1 BIM Model Development

A LOD 300 model of a power plant was created in Revit, as shown in Fig. 7. The power plant had three separate units of the transformer (T), generator-turbine (G-T), boiler-feeder (B-F), conveyer, electro-static-precipitator (ESP) and natural draught cooling towers (NDCT). However, a single chimney was present for the whole power plant. The precast sections were only used in cooling towers. Apart from chimney and cooling towers, other buildings had mixed use of concrete and steel structures. Eight areas were identified as possible locations for temporary facilities (TF) and designated as TF1, TF2, ..., TF8. The construction was operated unit wise, and the total project duration was five years starting from 2 March 2020 onwards. The road network for this model had 161 nodes and 222 edges. The roads had 'asphalt', 'concrete', and 'earth' as pavement materials, and road width varied between 3 meters to 15 meters. Straight lines show the road connectors from TF locations to nearby existing roads with zero width. The pavement material and road width values are redundant for these roads. Fig. 8 depicts the road network, nodes naming, and material selection palette for a road segment. The temporary routes with overhead clashes were detected with a minimum height clearance requirement of 25 meters allowing the crane with the longest boom to pass after lowering the boom at an angle.

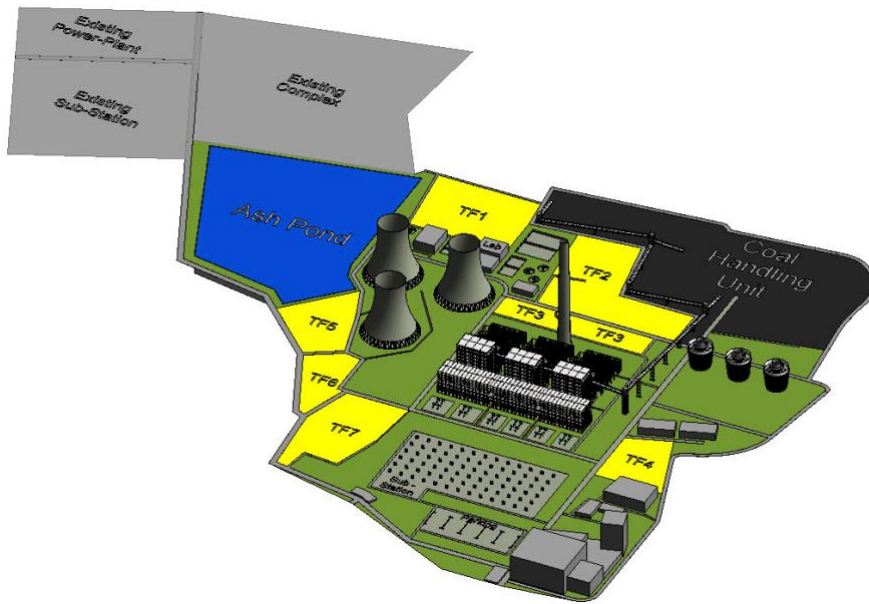


FIG. 7: LOD 300 model of thermal power plant project

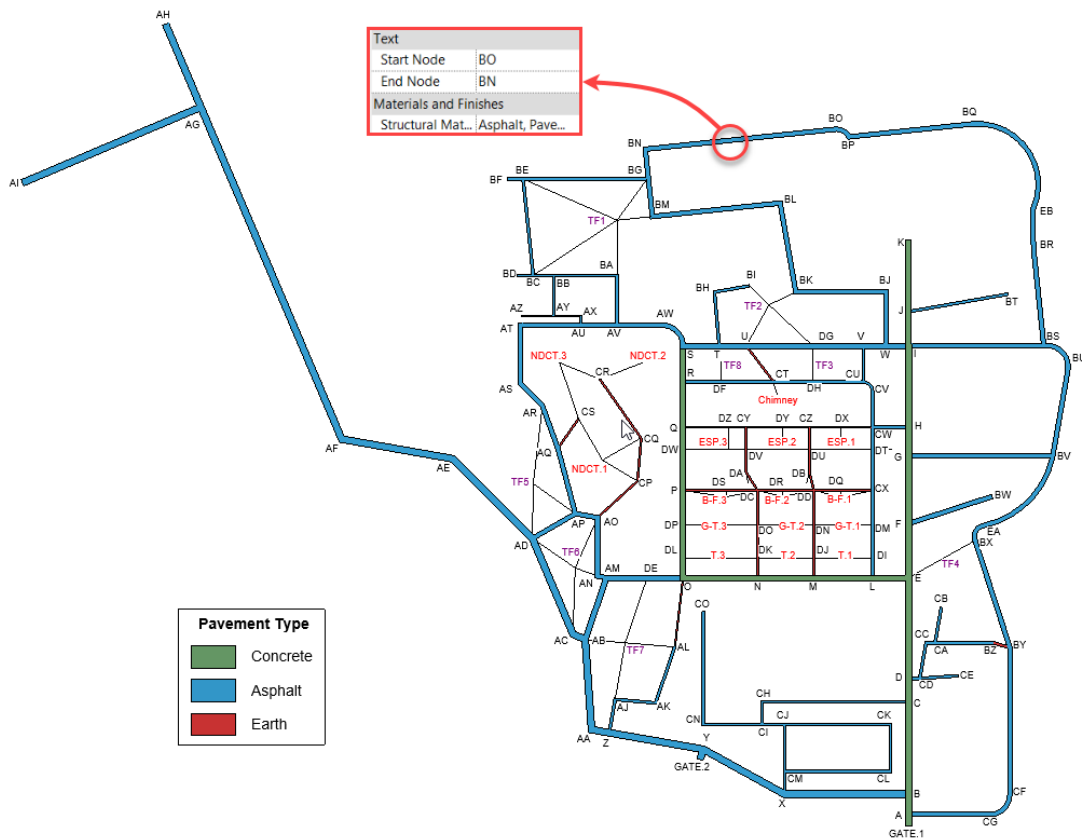


FIG. 8: Power plant road network and nodes naming, material selection palette for a road segment

4.2 Simulation Runs

Two model runs were carried out to present the possible outcomes from the complete process. The considerations for both tests are summarised in Table 1. In a state of no feasible route is found by the algorithm for the combination of chosen vehicles, that test run stood cancelled. The internal conflicts matrix and road network visualization were generated on the successful determination of all feasible routes.

TABLE 1: Test run 1 & 2 – considerations

Material Yard	Location		Vehicle Type		Hauling Capacity		Min Width (m)		Pavement Material	
	Test 1	Test 2	Test 1	Test 2	Test 1	Test 2	Test 1	Test 2	Test 1	Test 2
Concrete	TF2	TF2	transit mixer	transit mixer	6 m ³	6 m ³	3	3	None	None
Reinforcement	TF3	TF4	trailer	trailer	25 t	10 t	8	4	Earth	None
Excavation	TF8	TF5	dumper	dumper	15 m ³	15 m ³	3	3	None	None
Shuttering	TF6	TF6	wheel crane	wheel crane	20 t	20 t	6	6	None	None
Steel Work	TF7	TF7	crawler crane	trailer	200 t	10 t	6	4	Asphalt	None
Precast	TF1	TF1	trailer	trailer	10 t	10 t	4	4	None	None

Test 1 Check date = 18/12/2022 & Test 2 Check date = 31/10/2020

The material yards required throughout the project lifecycle were precast, concrete, reinforcement, excavation, shuttering and steelwork yard. The available equipment at the site were transit mixers, trailers, crawler cranes, wheel cranes and dumper. The main difference in considerations between test run 1 and test run 2 is the choice of equipment. As the equipment type changes, the minimum width and pavement type requirement also change. The available location for temporary facilities were eight. However, the facilities required were only 6. Hence, ‘TF5’ and ‘TF4’ were kept vacant in the first run, and ‘TF3’ and ‘TF8’ were kept vacant in the second run. Such scenarios are considered to take into account the accessibility of these available locations. The two runs were also performed on two different dates to see the difference in demand on the site. An additional test is done after the completion of any of these two runs. In this case, the road segment ‘AS - AT’ was blocked to see the variation in the outputs of routes. For the second objective, a scenario was considered when the concrete supply was required at the precast yard from an external ready-mix concrete plant due to the high demand for concrete at the site. Hence, relating to Fig. 8 and Table 1, the start and terminating nodes for this movement were ‘GATE.1’ and ‘TF1’. The equipment chosen for movement is a ‘transit mixer’, and results were generated for all possible conflicts count.

5. RESULTS AND DISCUSSION

The runs conducted on specified dates filtered the ongoing activities at the site and generated the supply-demand points as shown in Tables 2 & 3. As the precast activity was ongoing in the first case, the precast yard is found as demand points for reinforcement and concrete yard. However, for run 2 (dated 31/10/2020), even though precast activity was not in progress, the developed approach accounted for the future supply to the precast yard at TF1; it is due to the check date for run 2 is before the run 1 check date (18/12/2022). In both the runs, it was found that the precast yard located at ‘TF1’ is the delivery point for both the concrete yard and reinforcement yard. For other material yards, the changes and increase in the demand points can be observed from Table 3 to Table 2. However, In 2020 October, the chimney had a demand for reinforcement and concrete. Whereas, by December 2022, the chimney construction is supposed to be completed. Hence, it has no demand left after two years. The feasible shortest routes were generated using these data.

TABLE 2: Feasible routes for internal movements for run 1

Material Yard	Supply Point	Demand Point	Length (m)	Route
Precast	TF1	NDCT (Unit 2)	1425.043	TF1 - BA - AV - AU - AT - AS - AR - AQ - AP - AO - CP - CQ - CR - NDCT (Unit 2)
Concrete	TF2	NDCT (Unit 1)	1118.252	TF2 - U - T - S - AW - AV - AU - AT - AS - AR - AQ - CS - NDCT (Unit 1)
		NDCT (Unit 2)	1555.908	TF2 - U - T - S - R - Q - DW - P - DP - DL - O - DE - AM - AN - AO - CP - CQ - CR - NDCT (Unit 2)
		NDCT (Unit 3)	1143.443	TF2 - U - T - S - AW - AV - AU - AT - AS - AR - AQ - CS - NDCT (Unit 3)
		TF1	629.780	TF2 - BK - BL - BM - TF1
Reinforcement	TF3	NDCT (Unit 1)	Infinite	-
		NDCT (Unit 2)	Infinite	-
		NDCT (Unit 3)	Infinite	-
		TF1	733.817	TF3 - DG - U - T - S - AW - AV - BA - TF1
Shuttering	TF6	NDCT (Unit 2)	533.191	TF6 - AO - AP - AQ - CS - NDCT (Unit 2)
Steelwork	TF7	ESP (Unit 2)	Infinite	-



TABLE 3: Feasible routes for internal movements for run 2

Material Yard	Supply Point	Demand Point	Length (m)	Route
Concrete	TF2	Chimney	243.114	TF2 - U - CT - Chimney
		NDCT (Unit 1)	1118.252	TF2 - U - T - S - AW - AV - AU - AT - AS - AR - AQ - CS - NDCT (Unit 1)
		TF1	629.780	TF2 - BK - BL - BM - TF1
Reinforcement	TF4	Chimney	859.764	TF4 - E - F - G - H - CW - CV - CU - DH - CT - Chimney
		NDCT (Unit 1)	1126.810	TF4 - E - L - M - N - O - DE - AM - AN - AO - CP - NDCT (Unit 1)
		TF1	1468.096	TF4 - E - F - G - H - CW - CV - CU - DH - CT - U - T - S - AW - AV - BA - TF1
Shuttering	TF6	NDCT (Unit 1)	332.462	TF6 - AO - CP - NDCT (Unit 1)
Steelwork	TF7	B-F (Unit 1)	777.820	TF7 - DE - O - N - DK - DO - DC - DR - DD - B-F (Unit 1)

Due to the choice of vehicle and available road network, it can be observed that 36% of the supply will not reach the destination in Table 2. In test 1, at ‘TF3’, the vehicle selected for delivery from the reinforcement yard was a trailer of a hauling capacity of 25 tonnes. However, due to the vehicle type and load constraints, its movement was restricted on the earthen road, and the distance reported was infinite. As shown in Fig. 8, the roads joining ‘NDCT’ (i.e., AO-CP, CP-CQ, CQ-CR and AQ-CS) are earthen. The possible way out from no feasible routes is changing the equipment type, hauling capacity, pavement material, or relocating the material yards at a different location. For the transit mixer from the concrete yard at ‘TF2’ and the wheel crane from shuttering yard at ‘TF6’, all the destinations were reachable. The length of routes with route direction is mentioned in columns 4 and 5 of Table 2. However, in the case of steelwork from ‘TF7’, the trip cannot be completed to nodes ‘DE’, ‘AB’ or ‘AJ’ as all these roads are asphalt roads, whereas the choice of equipment is a crawler crane. The road segment connecting between ‘AL’ and ‘O’ is an earthen road, but the road width of 3 meters does not permit the crane to move through. Hence, a crawler crane cannot be a choice for transporting materials from steelyard in this specific site layout.

According to the database, the wheel crane does not have any pavement type constraint. So, at the end of the first run, few changes were made in the choice of equipment to ensure the feasible flow of materials between supply and demand points, as shown in Table 1. First, the hauling capacity of the trailer was decreased for the reinforcement yard from 25 tonnes to 10 tonnes, which removed the restriction of its movement on earthen roads. Trailers with similar specifications were also assigned to the steelyard. These modifications made all the movements possible in run 2, as summarised in Table 3. As feasible routes were not found out for run 1, it was terminated hereafter. Once the feasible routes in run 2 were calculated, the traffic flow through road segments and the internal conflicts matrices were generated. Next, the condition for the external supply transit mixer coming to the site was simulated to generate the number of possible conflicts with internal movements. The number of conflicts found against the shortest route from ‘GATE.1’ to ‘TF1’ for the external vehicle is 211. A Pareto front in Fig. 9 illustrates the inverse relationship between the distance to be traversed and possible conflicts. Once the total number of conflicts in a route crosses the maximum allowable conflict, equipment changes its path. It tries to find the alternate shortest route and records the conflicts faced on that road. For example, the route length for conflicts 40 to 88 is 2394.316 meters, which means if this route were chosen, conflicts encountered would be 40. The abrupt change of travel distance between conflicts 0 and 40 in Fig. 9 shows that solution for 40 conflicts may prove to be more economical than route having no conflicts; minimizing to 0 conflicts from 40 increases the distance for one trip in a single direction 506.295 meters. The user can check the distance and route according to maximum allowable conflict from Table 4.

However, if not satisfied with the results from the conflicts method, the user can identify a route based on the most congested roads. Fig. 10 represents a PCU-based heatmap visualization of the traffic flow at the site, with ‘red’ being the most congested roads to ‘green’ being the least congested. According to test run 2, a maximum PCU of 544 per day was acquired in the ‘U - TF2’ road segment. The heatmap colouring is based on this highest index and zero. In Fig. 10(a), the most critical road segment for timely project delivery can be observed at the given testing date. For example, if the user is willing to pass the external vehicle ‘transit mixer’ from ‘GATE.1’ to ‘TF1’ through roads with traffic up to 70% of the highest traffic flow, the feasible shortest route gets generated. The resulted path is ‘GATE.1 - A - B - C - D - E - F - G - H - CW - CV - CU - V - W - BJ - BK - BL - BM - TF1’ having a length of 2078.179 meters. It can be observed in Table 4 that the result generated is a route having 143 conflicts. Hence, this route can prove to be one of the economic routes. Fig. 11 represents two routes with different values of

maximum allowable flows. The cyan lines represent the non-used routes, and the magenta lines represent the feasible route taken by the transit mixer.

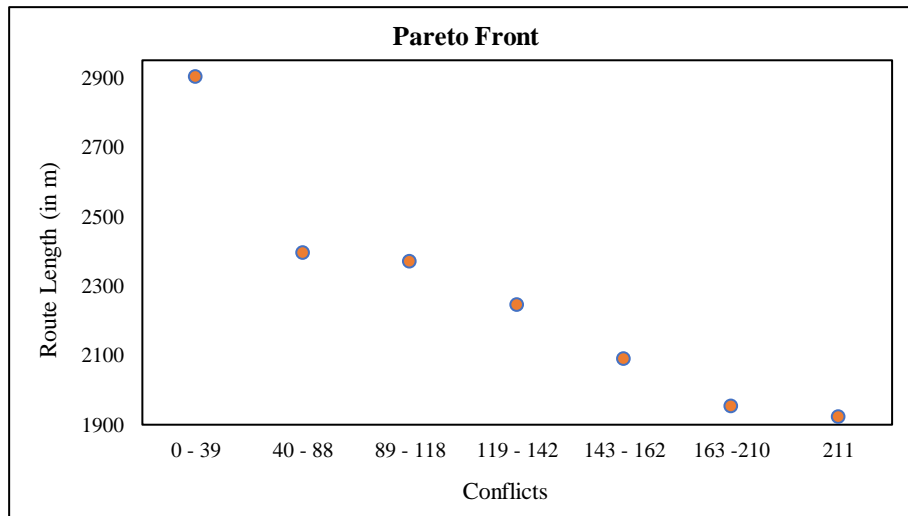


FIG. 9: Pareto front between conflicts and route length for test run 2

TABLE 4: Results of Pareto front between conflicts and route length for test run 2

Conflicts	Length (m)	Route
0 - 39	2900.611	GATE.1 - A - CG - CF - BY - BX - EA - BV - BU - BS - BR - EB - BQ - BP - BO - BN - BG - TF1
40 - 88	2394.316	GATE.1 - A - B - X - Y - Z - AA - AB - AC - AD - AP - AQ - AR - AS - AT - AU - AX - AY - BB - BC - TF1
89 - 118	2369.431	GATE.1 - A - B - X - Y - Z - AA - AB - AM - AN - AO - AP - AQ - AR - AS - AT - AU - AX - AY - BB - BC - TF1
119 - 142	2245.183	GATE.1 - A - B - X - Y - Z - AA - AB - AM - AN - AO - AP - AQ - AR - AS - AT - AU - AV - BA - TF1
143 - 162	2089.179	GATE.1 - A - B - C - D - E - F - G - H - CW - CV - CU - V - W - BJ - BK - BL - BM - TF1
163 - 210	1951.697	GATE.1 - A - B - C - D - E - L - M - N - DK - DO - DC - DA - DV - CY - DZ - Q - R - S - AW - AV - BA - TF1
211	1921.748	GATE.1 - A - B - C - D - E - L - DI - DM - CX - DT - CW - CV - CU - DH - CT - U - T - S - AW - AV - BA - TF1

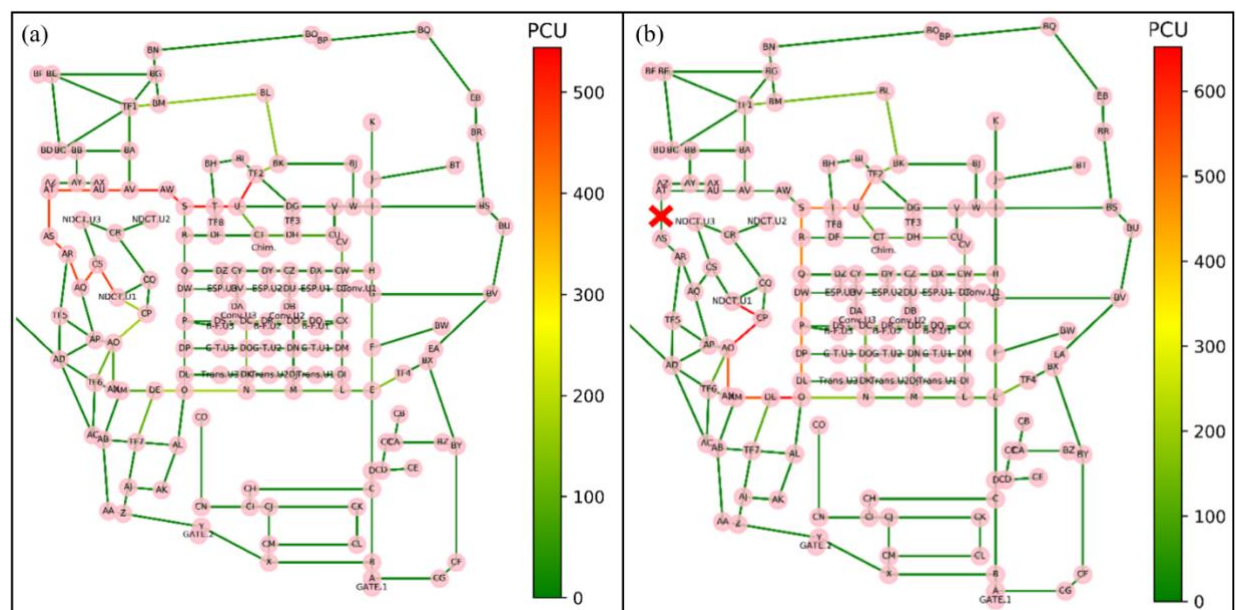


FIG. 10: Traffic flow representation through heatmap: (a) in normal condition, (b) when road AS - AT is blocked

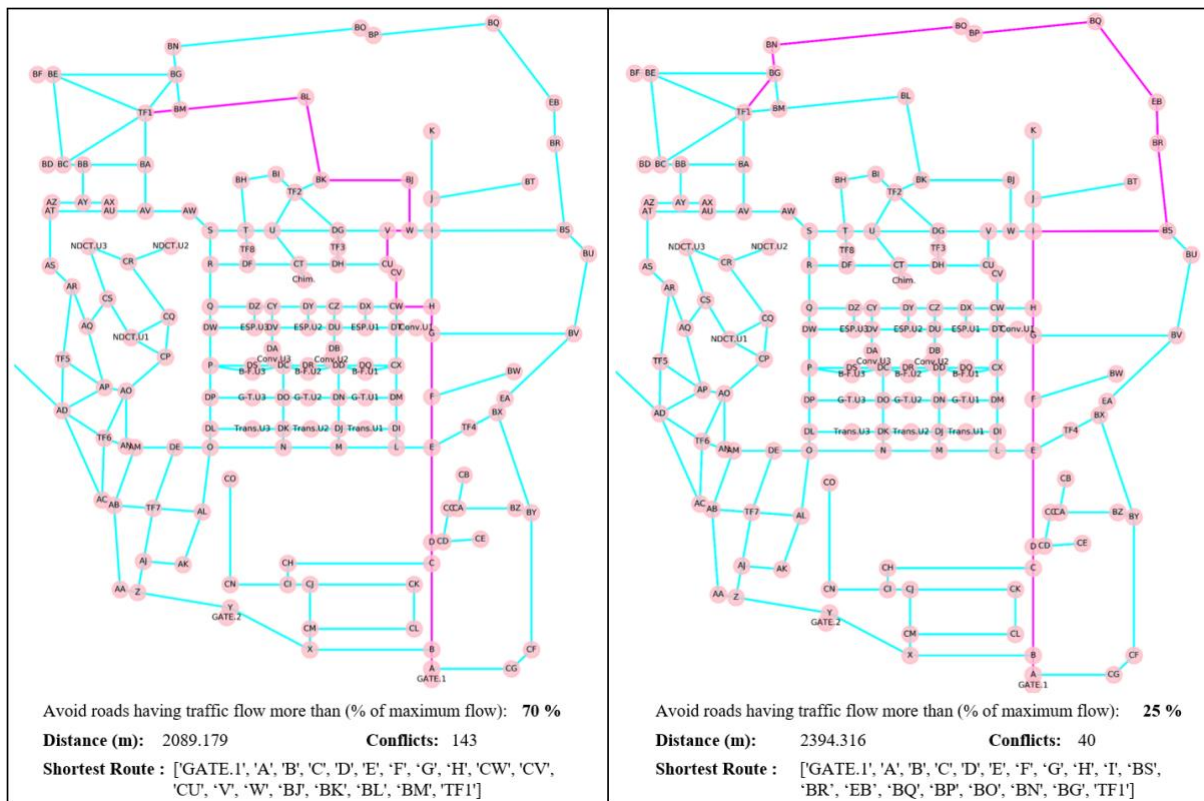


FIG. 11: Routes based on the percentage of maximum allowable traffic flow

As the planner looks forward to the weekly look ahead plans, the routes shown might not be available for use due to sudden equipment breakdowns. Such a scenario was generated when the road AS - AT is considered to be blocked. Fig. 10(b) shows the new most crucial road segments for the construction site. The variation in PCU/day values can be observed as well. The increase happened because of the new overlaps in equipment paths for the segments 'AN - AO', 'AO - CP', and 'CP - NDCT.Unit1'.

This optimization module is efficient in the case of $n < e$, as it increases the combinations of road segments possible to be chosen for a trip. It helps in minimizing the human effort required in understanding and interpreting multiple constraints along with segment distances when determining the minimum route.

6. CONCLUSION

BIM proved to be beneficial in the integration of site route planning and accessibility to enhance the construction site logistics. This study targeted the shortest feasible route and minimizing the conflict and congestion at the site. The study contributes to the body of knowledge through a systematic framework for integrating BIM and construction schedules for site route planning. The possibility of creating an automated 4D schedule through standardized string-based search is also presented. Also, a mathematical model for equivalent PCU to calculate probabilistic conflicts at intersections is proposed, which accounts for heavy equipment movement on the construction site. The day-to-day interactive nature of the model captures a better understanding of the dynamic site situation even before the start of the project. The project planners can benefit from the developed workflow in assigning routes between supply and destination facilities on a daily basis to reduce possible conflicts and enhance accessibility. Finally, the results from the optimization module are aided with visualization in the mode of network graph to enhance the understanding of the planners. To achieve a safe work environment at the site, the movement conflicts of site personnel with plant and machinery can be integrated with future research in this domain. The project supply chain can be improved by integrating the developed workflow with the pre-scheduled lead supply vehicles. Further, the possibility of dynamically assigning the internal movement routes of equipment can be explored by the assigned priority index of temporary facilities. The applicability of the developed workflow can be further enhanced by embedding it with facilities layout planning to address the complete SLP problem of the construction site.

REFERENCES

- Adrian, A.M., Utamima, A. and Wang, K.J. (2015) 'A comparative study of GA, PSO and ACO for solving construction site layout optimization', *KSCE Journal of Civil Engineering*, 19(3), pp. 520–527. doi:10.1007/s12205-013-1467-6.
- Akinci, B., Fischer, M. and Kunz, J. (2002) 'Automated generation of work spaces required by construction activities', *Journal of Construction Engineering and Management*, 128(4), pp. 306–315. doi:10.1061/(ASCE)0733-9364(2002)128:4(306).
- Ali, M.S.A.D., Babu, N.R. and Varghese, K. (2005) 'Collision Free Path Planning of Cooperative Crane Manipulators Using Genetic Algorithm', *Journal of Computing in Civil Engineering*, 19(2), pp. 182–193. doi:10.1061/(ASCE)0887-3801(2005)19:2(182).
- Andayesh, M. and Sadeghpour, F. (2014) 'The time dimension in site layout planning', *Automation in Construction*, 44, pp. 129–139. doi:10.1016/j.autcon.2014.03.021.
- Barlish, K. and Sullivan, K. (2012) 'Automation in Construction How to measure the benefits of BIM — A case study approach', *Automation in Construction*, 24, pp. 149–159. doi:10.1016/j.autcon.2012.02.008.
- Benjaoran, V. and Peansupap, V. (2019) 'Grid-based construction site layout planning with Particle Swarm Optimisation and Travel Path Distance', *Construction Management and Economics*, 0(0), pp. 1–16. doi:10.1080/01446193.2019.1600708.
- Brand, M. *et al.* (2010) 'Ant Colony Optimization Algorithm for Robot Path Planning', in *2010 International Conference On Computer Design And Applications*. doi:10.1109/TCSET.2018.8336181.
- CSIR (2017) *Indian Highway Capacity Manual (Indo-HCM)*. Available at: https://www.crridom.gov.in/sites/default/files/Indo-HCM_Snippets.pdf.
- Fazli, A. *et al.* (2014) 'Appraising Effectiveness of Building Information Management (BIM) in Project Management', *Procedia Technology*, 16, pp. 1116–1125. doi:10.1016/j.protcy.2014.10.126.
- Harris, F. and McCaffer, R. (2013) *Modern Construction Management*. John Wiley & Sons.
- Karmakar, A. and Delhi, V.S.K. (2021) 'Construction 4.0: what we know and where we are headed?', *Journal of Information Technology in Construction (ITcon)*, 26(July), pp. 526–545. doi:10.36680/j.itcon.2021.028.
- Kumar, S.S. and Cheng, J.C.P. (2015) 'Automation in Construction A BIM-based automated site layout planning framework for congested construction sites', *Automation in Construction*, 59, pp. 24–37. doi:10.1016/j.autcon.2015.07.008.
- Lam, K.C., Ning, X. and Ng, T. (2007) 'The application of the ant colony optimization algorithm to the construction site layout planning problem', *Construction Management and Economics*, 25(4), pp. 359–374. doi:10.1080/01446190600972870.
- Le, P.L., Dao, T. and Chaabane, A. (2019) 'Multi-Objective Construction Site Layout Optimization using BIM', in *In Conference Proc.*
- Li, H. and Love, P.E.D. (2000) 'Genetic search for solving construction site-level unequal-area facility layout problems', *Automation in Construction*, 9(2), pp. 217–226.
- Li, H. and Peter E. D. Love (1998) 'Site-Level Facilities Layout using Genetic Algorithms', *Computing in civil engineering*, 12(October), pp. 227–231.
- Li, X., Xu, J. and Zhang, Q. (2017) 'Research on Construction Schedule Management Based on BIM Technology', *Procedia Engineering*, 174, pp. 657–667. doi:10.1016/j.proeng.2017.01.214.
- Li, Z. *et al.* (2001) 'A procedure for quantitatively evaluating site layout alternatives A procedure for quantitatively evaluating site layout alternatives', *Construction Management and Economics*, 19(5), pp. 459–467. doi:10.1080/01446190110044825.
- Lin, J.J.C. *et al.* (2013) 'Accessibility evaluation system for site layout planning – a tractor trailer example', *Visualization in Engineering*, 1(1), pp. 1–11. doi:10.1186/2213-7459-1-12.



- Lin, J.J.C., Hung, W.H. and Kang, S.C. (2015) 'Motion Planning and Coordination for Mobile Construction Machinery', *Journal of Computing in Civil Engineering*, 29(6), pp. 1–13. doi:10.1061/(ASCE)CP.1943-5487.0000408.
- Mahdjoubi, L. and Yang, J.L. (2001) 'An intelligent materials routing system on complex construction sites', *Logistics Information Management*, 14(5/6), pp. 337–344. doi:10.1108/09576050110404422.
- Mawdesley, M.J., Al-jibouri, S.H. and Yang, H. (2002) 'Genetic Algorithms for Construction Site Layout in Project Planning', *Journal of Construction Engineering and Management*, 128(5), pp. 418–426. doi:10.1061/(ASCE)0733-9364(2002)128.
- Neitzel, R.L., Seixas, N.S. and Ren, K.K. (2001) 'A Review of Crane Safety in the Construction Industry', *Applied Occupational and Environmental Hygiene*, 16(12), pp. 1106–1117. doi:10.1080/10473220127411.
- Ning, X., Lam, K.C. and Lam, M.C.K. (2010) 'Dynamic construction site layout planning using max-min ant system', *Automation in Construction*, 19(1), pp. 55–65. doi:10.1016/j.autcon.2009.09.002.
- Pradhananga, N. and Teizer, J. (2013) 'Automatic spatio-temporal analysis of construction site equipment operations using GPS data', *Automation in Construction*, 29, pp. 107–122. doi:10.1016/j.autcon.2012.09.004.
- Pradhananga, N. and Teizer, J. (2014) 'Congestion Analysis for Construction Site Layout Planning using Real-time Data and Cell-based Simulation Model', *Computing in Civil and Building Engineering*, pp. 955–1865.
- Sadeghpour, F., Moselhi, O. and Alkass, S.T. (2006) 'Computer-Aided Site Layout Planning', *Journal of Construction Engineering and Management*, 132(2), pp. 143–151. doi:10.1061/(ASCE)0733-9364(2006)132:2(143).
- Sanad, H.M., Ammar, M.A. and Ibrahim, M.E. (2008) 'Optimal Construction Site Layout Considering Safety and Environmental Aspects', *Journal of Construction Engineering and Management*, 134(7), pp. 536–544. doi:10.1061/(ASCE)0733-9364(2008)134.
- Schwabe, K., König, M. and Teizer, J. (2016) 'BIM Applications of Rule-Based Checking in Construction Site Layout Planning Tasks', in *33rd International Symposium on Automation and Robotics in Construction*, pp. 209–217. doi:10.22260/ISARC2016/0026.
- Singh, A.R. and Delhi, V.S.K. (2018) 'User behaviour in AR-BIM-based site layout planning', *International Journal of Product Lifecycle Management*, 11(3), pp. 221–244. doi:10.1504/IJPLM.2018.094715.
- Singh, A.R., Karmakar, A. and Delhi, V.S.K. (2020) 'Decision Support System for Site Layout Planning', in *Proceedings of the 37th International Symposium on Automation and Robotics in Construction (ISARC)*, pp. 1008–1013. doi:10.22260/ISARC2020/0139.
- Singh, A.R., Patil, Y. and Delhi, V.S.K. (2019) 'Optimizing Site Layout Planning utilizing Building Information Modelling', in *Proceedings of the International Symposium on Automation and Robotics in Construction*, pp. 376–383.
- Singh, V. and Helander, D. (2016) 'BIM in building renovation projects : What is the useful minimum information requirement?', *International Journal of Product Lifecycle Management*, 9(1), pp. 65–86. doi:10.1504/IJPLM.2016.078863.
- Soltani, A.R. and Fernando, T. (2004) 'A fuzzy based multi-objective path planning of construction sites', *Automation in Construction*, 13(6), pp. 717–734. doi:10.1016/j.autcon.2004.04.012.
- Soltani, A.R., Tawfik, H. and Fernando, T. (2002) 'A multi-criteria based path finding application for construction site layouts', *Proceedings of the International Conference on Information Visualisation*, 2002-Janua, pp. 779–784. doi:10.1109/IV.2002.1028868.
- Song, S. and Marks, E. (2019) 'Construction Site Path Planning Optimization through BIM', *Computing in Civil Engineering 2019: Visualization, Information Modeling, and Simulation - Selected Papers from the ASCE International Conference on Computing in Civil Engineering 2019*, (June), pp. 369–376. doi:10.1061/9780784482421.047.

- Tam, C.M. and Tong, T.K.L. (2003) 'GA-ANN model for optimizing the locations of tower crane and supply points for high-rise public housing construction', *Construction Management and Economics*, 21(3), pp. 257–266. doi:10.1080/0144619032000049665.
- Turky, A. *et al.* (2013) 'Path planning with obstacle avoidance based on visibility binary tree algorithm', *Robotics and Autonomous Systems*, 61(12), pp. 1440–1449. doi:10.1016/j.robot.2013.07.010.
- UNIFI (2019) *BIM Software: Which is the Most Popular?* Available at: <https://unifilabs.com/BIM-software> (Accessed: 21 July 2021).
- Varghese, K. and O'Connor, J.T. (1995) 'Routing large vehicles on industrial construction sites', *Journal of Construction Engineering and Management*, 121(1), pp. 1–12. doi:10.1061/(ASCE)0733-9364(1995)121:1(1).
- Zuppa, D., Issa, R.R.A. and Suermann, P.C. (2009) 'BIM's Impact on the Success Measures of Construction Projects', *Computing in Civil Engineering*, pp. 503–512.